


RESEARCH ARTICLE | AUGUST 22 2017

Life-cycle analysis of photovoltaic systems in Hong Kong

Siwei Lou ; Danny H. W. Li; Wilco W. Chan; Joseph C. Lam



J. Renewable Sustainable Energy 9, 045901 (2017)

<https://doi.org/10.1063/1.4999596>



Articles You May Be Interested In

Life cycle assessment of hole transport free planar–mesoscopic perovskite solar cells

J. Renewable Sustainable Energy (March 2020)

Analysis of feed-in tariff models for photovoltaic systems in Thailand: An evidence-based approach

J. Renewable Sustainable Energy (July 2019)

Cost management for waste to energy systems using life cycle costing approach: A case study from China

J. Renewable Sustainable Energy (March 2016)



Special Topics Open for Submissions

[Learn More](#)

Life-cycle analysis of photovoltaic systems in Hong Kong

Siwei Lou,^{1,a)} Danny H. W. Li,¹ Wilco W. Chan,² and Joseph C. Lam¹

¹*Building Energy Research Group, Department of Architecture and Civil Engineering, City University of Hong Kong, Tat Chee Avenue, Kowloon, Hong Kong, China*

²*School of Hotel and Tourism Management, the Hong Kong Polytechnic University, Hung Hom, Kowloon, Hong Kong, China*

(Received 26 April 2017; accepted 7 August 2017; published online 22 August 2017)

This paper studied the payback period of grid-connected photovoltaic (PV) panels by the net present value method. The PV performance data were acquired by on-site measurements of two rooftop projects in subtropical Hong Kong. The sensitivity of various variables to the payback period was evaluated by the Extended Fourier Amplitude Sensitivity Test. The monetary payback periods were evaluated at different values of the most relevant variables and compared with the embodied energy and greenhouse gas payback periods. The PV panels of the two projects produced 122–143 kWh/m² electricity per year in Hong Kong, which saved 139–163 HKD electricity tariff per square meter per year. The sensitivity analysis showed that the monetary payback period was sensitive to the initial cost and tariff increase rate uncertainties. The PV monetary payback period varied from 13.4 to 16.8 years at different tariff increase rates and investment costs, based on the current carbon trading benefit. The monetary payback period was much greater than the embodied energy and greenhouse gas payback periods, which were 10.8–12.7 years and 5.3–6.2 years, respectively. Implications of the payback period differences were discussed. *Published by AIP Publishing.* [<http://dx.doi.org/10.1063/1.4999596>]

I. INTRODUCTION

There is a growing concern about the energy use and its likely adverse effects on the environment. The electricity generation of Hong Kong relies on fossil fuels and nuclear energy imported from Mainland China (To *et al.*, 2012). The combustion of fossil fuels is the main source of greenhouse gas (GHG), air pollutant emissions, climate change, and respiratory illnesses (Oliver *et al.*, 2015). The local electricity tariff increases, probably due to the gradually exhausting fuel reserves in the world. Recently, the local Environment Bureau (2015) has proposed an energy-saving plan. The plan requires that renewable energy shall provide at least 1% of electricity consumption for lighting and power in new school buildings. To meet the ever-increasing demands for energy and the consensus of eco-protection, electricity generation by renewable techniques can be clean and safe alternatives to fossil fuels (Akinyele and Rayudu, 2016a; Hennecke *et al.*, 2013; and Islam *et al.*, 2013). A promising approach is installing photovoltaic (PV) panels to harvest solar energy (Li *et al.*, 2013a; 2013b; and Sweeney *et al.*, 2016).

Solar availability in Hong Kong is good and, in theory, has high PV application potential (Lam and Li, 1996; Li *et al.*, 2015; and Wong *et al.*, 2016). In practice, however, the PV panels can be costly, space demanding, and thus unpopular, which requires significant subsidy push to meet high installation targets (Shukla and Chaturvedi, 2012). Besides, the PV performance in operation can be different from its nameplate efficiency in the standard test conditions (Skoplaki and Palyvos, 2009). There were many previous works on the PV monetary and embodied energy payback (Akinyele, 2017; Akinyele and Rayudu, 2016b; Akinyele and

^{a)} Author to whom correspondence should be addressed: swlou2-c@my.cityu.edu.hk

Rayudu, 2016c; Bhakta *et al.*, 2015; Hasanuzzaman *et al.*, 2015; and Nawaz and Tiwari, 2006), but most of the works examined the PV cell performance under different solar radiation and energy output assumptions. The assumed solar energy is flexible to supporting comprehensive studies in various climates; however, on-site measurements would be the proper and reliable approach for evaluating the performance in practice (Li *et al.*, 2012). KolokotsaKolhe *et al.* (2002) focused on the expenditure analysis of standalone PV rather than the cost-benefit trade-offs. Sharma and Tiwari (2013) implemented a comprehensive PV energy and cost analysis. However, the monetary benefit from carbon trading, as a policy encouragement to PV installation, was not studied. This study was about the economic benefit of grid-connected building integrated PV (BIPV) systems in Hong Kong based on the field measurement of solar irradiance and electricity generation from 2010 to 2015. Two different PV systems were studied, and a comparison was made between them. The systems will provide essential on-site measurement data to local and international PV system designs. Besides, the monetary benefit was analyzed by the net present value that considers the time value of money and electricity tariff variations over years. The sensitivity analysis studied the impact of various causes to the PV monetary payback period, including the change in monetary investment, electricity tariff, carbon trading, maintenance cost, inflation, and interest rate. The monetary payback periods under different economic conditions were analyzed. The payback periods of embodied energy and greenhouse gas were also studied to evaluate the life-cycle impact of PV applications in energy saving and environment protection. The findings and implications are discussed.

II. INFORMATION ON THE PV SYSTEM AND SITE

We studied the PV panels of two sites in Hong Kong (22.3N, 114.2E) with a hot and humid climate. The panels of site A were installed on the opaque roof of a low-rise school building at a low densely built area. The panels of site B composed part of a high-rise institutional building skylight in the downtown. The two sites represent the usual building integrated PV installation scenarios that may influence the PV performance. The silicon PV panels of both sites were rarely obstructed by the surrounding buildings. Table I gives the technical details of the PV panels under standard test conditions (i.e., cell temperature = 25 °C, solar irradiance = 1 kW/m², and air mass = 1.5). The panels in both sites had slight tilt angles to prevent dust and rainwater accumulation. There were tilt angle adjustments of the PV cells in site A throughout the measurement period for secondary school educations and undergraduate studies. Referring to the local latitude, the tilt angle was less than 23°, while no detailed record was made. The tilt angle of cells in site B was fixed and less than 12°. Solar energy on the PV cells of such a low tilt angle was assumed to be the same as the horizontal solar energy for simplicity. A previous study showed that the annual Global solar irradiance (GSR) difference between a 23°-tilt plane and the horizontal surface was less than 5%. There were 12 and 224 modules in

TABLE I. Technical specifications of the solar cell.

		Site A	Site B
Peak voltage for each module		17 V	35.4 V
Peak current for each module		4.9 A	4.95 A
Peak module wattage		83 W	175 W
Maximum power point temperature coefficient	Current ($\alpha_{I, m}$)	0.06%/K	−0.43%/K
	Voltage ($\alpha_{V, m}$)	−155 mV/K	−145 mV/K
	Power ($\alpha_{P, m}$)	−0.05%/K	−0.7%/K
Module nameplate efficiency		14.2%	13.3%
Tilt and azimuth		Less than 23°, Southwest	4°–12°, different azimuthal directions
Number of modules		12	224
Total area		6.75 m ²	296 m ²
Total weight		96 kg	4077 kg

sites A and B, which were 6.75 m^2 and 296 m^2 , respectively. Both systems fed power to the grid when there were surpluses in power generations or obtained power from the grid when the on-site generation was not enough. No battery was needed for energy storage.

III. THE PV PERFORMANCE

Since climatic variables, including solar irradiance and panel temperature, may influence the PV panel performance, the field measurement is the most reliable method of collecting relevant data to evaluate the PV performance in the actual operating environment. In this study, PV power production data from January 2011 to December 2015 were used for the analysis. The solar irradiance data were recorded by a local weather station (Hong Kong Observatory, HKO) every hour. The power productions were recorded every 5–10 min and converted into hourly data for the subsequent analysis. It is inevitable that there were periods of data missing or error although significant efforts were made to keep the recording continuous and in good conditions. In total, 19 541 and 15 108 groups of hourly recordings were acquired from sites A and B, respectively. The missing data of site B were mainly from January to June of both 2011 and 2015.

A. Power output and efficiencies

Figure 1 plots the monthly average daily horizontal global solar radiation and PV electricity output by the measurements. The PV energy output of both sites varied consistently with the solar irradiance. The daily solar radiation ranged from 2564 Wh/m^2 in February to 5366 Wh/m^2 in July. The solar radiation agreed with our previous findings (Li *et al.*, 2015). The daily PV energy output of sites A and B varied from 260 Wh/m^2 and 306 Wh/m^2 in February to 429 Wh/m^2 and 485 Wh/m^2 in summer months. The greatest daily solar radiation and energy output in July or August were because of the long daytime and high solar altitude in summer. The below-average records from November to March were due to the low solar altitude angle in winter and unstable weather conditions in spring. Holistically, the average yearly energy productions were 143 kWh/m^2 for site A and 122 kWh/m^2 for site B. Referring to Akinyele and Rayudu (2016b), we define the energy loss as the difference between the energy output of sites at the nameplate and measured efficiencies. Considering the annual solar radiation of 1401 kWh/m^2 and the nameplate efficiencies, the annual energy loss was 55.9 kWh/m^2 for site A and 64.3 kWh/m^2 for site B due to the difference between the actual outdoor environment and STD. Assuming a typical PV cell lifespan in the range of 20–30 years and a yearly degradation rate of 0.5%, the lifecycle energy output of PV cells ranged from 2714.5 to 3973 kWh/m^2 for site A and 2315.9 to 3389.6 kWh/m^2 for site B. The lifecycle energy loss ranged from 17 173 to 25 858 for site A and 16 311 to 24 550 for site B due to the different outdoor working environment and cell aging. Considering that the annual energy usage of university and secondary school was 209 kWh/m^2 and 59 kWh/m^2 (EMSD,

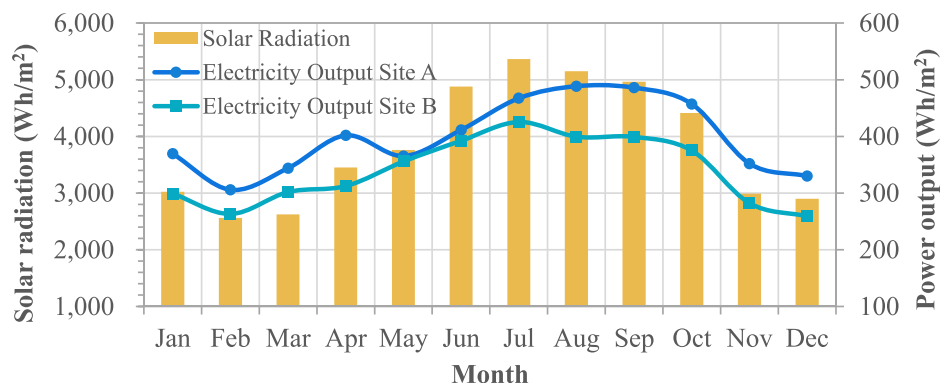


FIG. 1. The monthly average daily horizontal solar radiation and PV electricity production.

2016), respectively, it requires 1.46%–1.71% of the university construction area and 0.41%–0.48% of the secondary school construction area to cover 1% of their annual electricity usage.

The efficiencies can be employed to evaluate the electricity output of PV in different installations. Figure 2 gives the monthly and overall average efficiencies of the two sites from 2011 to 2015. The horizontal solar radiation determined the efficiencies since the global solar radiation on the horizontal and slightly tilted planes differs by 5% for Hong Kong (Li and Lam, 2007). The overall efficiencies of PV panels (η) in sites A and B were 10.1% and 8.6%, respectively, which were significantly less than their nameplate efficiencies of 14.2% and 13.3%, respectively, due to the differences between the test and operation conditions. The monthly efficiencies were greater than the overall efficiencies from November to April when the cell temperature was lower than the summer seasons. Compared with the hot summer, efficiencies in winter and early spring were closer to the design-values since the outdoor environment was closer to the Standard Test Condition. The greatest efficiency did not take place in the coldest months, January and February, probably because the PV cells are not sensitive to the low solar radiation and high sunlight incident angle during the period. Interestingly, the minimum monthly efficiency was in June for site A and in August for site B. The monthly efficiency profile difference can be explained by different cell installations and roof insulations of the two sites. The cells in the atrium skylight of site B may be influenced by the indoor air-conditioning, which leads to a rather flat efficiency variation curve from June to September of site B. The least efficiencies of 8.6% for site A and 7.7% for site B were found in summer seasons due to the high PV cell temperature. It is interesting to note that lower efficiency tended to coincide with the high daily solar radiation and power output during the summer months.

The frequency of occurrence (FOC) and cumulative FOC of the hourly PV efficiency are shown in Fig. 3, which gives a better idea about the operational efficiency during the 5-year monitoring period. The standard deviations of efficiencies were 9.7% for site A and 8.8% for site B. The first and third quartiles of the efficiencies were 6.3% and 13% for the panels in site A and 6.4% and 10.5% for site B. The 3rd quartiles of both sites were less than their respective nameplate efficiencies of 14.2% and 13.3%, which shows that the PV cells operated less than the nameplate efficiency in most circumstances throughout the year. The efficiency distribution of site A was more scattered than site B, which was probably due to the fact that the tilt angle adjustment of cells in site A leads to uncertainties in calculating its efficiency. Given that 50% of the data were within the first and third quartiles, the hourly efficiencies were clustered around the average efficiencies of 10.1% and 8.6%. The cumulative FOC shows that 50% and 30% of the hourly efficiencies were greater than 10% for the PV in sites A and B. The hourly efficiencies over 20% were probably due to the round-off error of the solar radiation measurements.

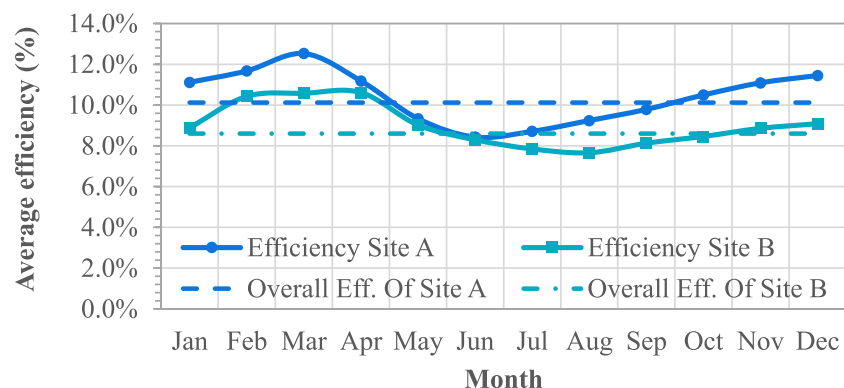


FIG. 2. The monthly and overall efficiency of the PV system from 2011 to 2015.

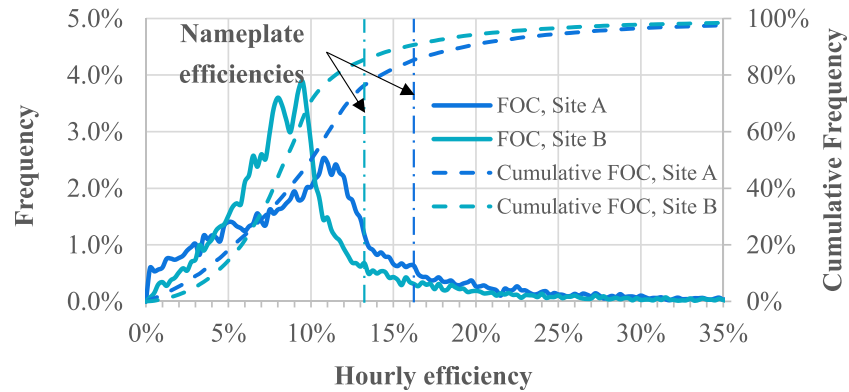


FIG. 3. Frequency of occurrence (FOC) for the PV system hourly efficiency for 2011–2015.

B. Hourly solar irradiance and PV power output

Average hourly solar irradiance, PV electricity output, and conversion efficiencies in the hot summer months of June, July, and August are presented in Figs. 4(a), 4(b), and 4(c), respectively. Figure 4(a) shows the horizontal solar irradiance that represents the solar energy on PV cells of low tilt angles in both sites, as discussed in Sec. II. The hourly data are essential to the studies of the maximum and variations of PV electricity output and its impact on the grid. It

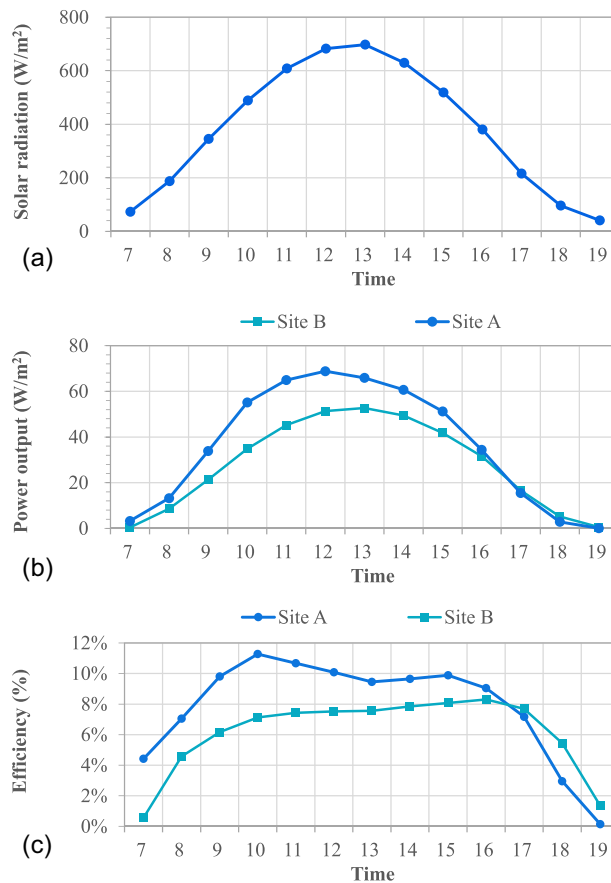


FIG. 4. (a) The average hourly horizontal solar irradiance for hot months from June to August. (b) The average hourly PV power output for hot months from June to August. (c) The average hourly efficiency of electricity conversion for hot months from June to August.

can be found in Figs. 4(a) and 4(b) that the irradiance and power output have similar profiles and are well matched owing to the proper data recording. The abundant solar irradiance and relatively high electricity output are because of the high solar altitude in summer. The peak solar irradiance was 697 W/m^2 , and the corresponding PV electricity output ranged from 53 W/m^2 to 69 W/m^2 in different sites. The average hourly efficiencies of the two sites were very different from their nameplate values. As given in Fig. 4(c), the low efficiencies of PV in both sites in the morning and afternoon were probably because the panels were not sensitive to the low solar irradiance at a high incident angle. It is worth pointing out that peak solar irradiance and hence significant solar heat gain tend to coincide with peak air conditioning requirements in the built environment. The findings implicated that the building integrated PV electricity production should be attractive to compensate the air-conditioning energy usage during peak cooling load hours in subtropical regions.

The average hourly efficiency was higher in the late morning than the late afternoon for site A, while it was quite symmetrical for site B. The difference was probably because the power temperature coefficient ($\alpha_{p, m}$ given in Table I) for site A is far less than that for site B (in absolute value). $\alpha_{p, m}$ closer to zero marks that there was less influence of PV cells in site A than site B when the solar irradiance and cell temperature started to rise in the morning. This explains the higher efficiency of site A in the morning than in the afternoon. The efficiency of PV cells on the opaque roof of site A decreased in the afternoon, which is probably due to the cell temperature increase during the day. Considering that PV cells of site B composed the skylight of an atrium, the high efficiency for PV cells in site B in the afternoon is likely because of the indoor-space air-conditioning.

IV. COST, ENERGY, AND ENVIRONMENTAL ANALYSIS

The monetary benefits of the PV system were depicted as the time that is needed to “return” the monetary investment by the benefits of PV in operation. A shorter payback period means that the initial cost can be returned in less time, and thus, the project is more attractive in the given financial conditions. The net present values (NPV) of the maintenance cost (M), the tariff saving (S), and the carbon emission trade benefit (T) in the N years of PV system operation were determined as follows (EMSD, 2007):

$$M = m \cdot \sum_{i=1}^N \left(\frac{1+e}{1+d} \right)^i, \quad (1)$$

$$S = s \cdot \sum_{i=1}^N \left(\frac{(1+e)}{(1+d)} (1-R) \right)^i, \quad (2)$$

$$T = t \cdot \sum_{i=1}^N \left(\frac{1-R}{1+d} \right)^i, \quad (3)$$

where m , s , and t in the lower case are the annual maintenance cost, tariff saving, and carbon emission trade benefit evaluated based on their current value; d and e are the real discount rate and electricity price escalation rate. Since the increase in both the electricity tariff and maintenance cost is somehow related to the increase in the cost of living, it is assumed that the rate of growth in the electricity tariff (e) is the same as the maintenance cost. R is the degradation rate of PV performance, which is assumed as 0.5% per year according to the median of the 1751 reports of silicon PVs summarized by Jordan and Kurtz (2013). The report covers different parts of the world, and thus, the degradation rate can be representative. The real discount rate (d) and the rate of electricity price increase (e) were determined as follows:

$$d = \frac{1+r}{1+r_{\text{inf}}} - 1, \quad (4)$$

$$e = \frac{1 + E}{1 + r_{\text{inf}}} - 1, \quad (5)$$

where r and E are the nominal interest rate and electricity price increasing rate, respectively; r_{inf} is the inflation rate. The “real” rates d and e give the relative variation speeds of nominal rates against the inflation rate.

The NPV of the PV system in operation for N years is given by

$$NPV = -C_0 - M + S + T. \quad (6)$$

The payback period is the time when the costs of initial investment and yearly maintenance are covered by the tariff saving and carbon trading benefits [NPV in Eq. (6) equals to zero]. The monetary payback period varies under different financial conditions and depends on the values of variables taken in Eqs. (1)–(6). The initial investment of PV installation (C_0) varies according to the type of PV panels, the cost of the labor force, the market of the PV product, and the scale of installation. The tariff saving (S), on the other hand, is largely dictated by the local tariff (s) and its rate of increasing (E) in the future. Although the current tariff is readily available, the government policies and fossil fuel market may influence its variation in future. The other variables of m , r , and r_{inf} may vary year by year due to various reasons. In this connection, the importance of different economic variables on the payback period should be evaluated by sensitivity analysis. The monetary payback period should be calculated based on the important variables taken at different values that represent various economic conditions.

A. Initial investment cost (C_0)

According to a report by the Lawrence Berkeley National Laboratory (Barbose *et al.*, 2015) based on 45 368 residential PV projects installed in 2014 in the United States, roughly 60% of the PV system installation costs ranged from 27.1 HKD(\$)/W to \$41.1/W. The report presented that the medium installation price of China was 45.2% of the United States, which was \$12.2/W–\$18.6/W for the present study. Considering that the nameplate efficiencies of PV in sites A and B were 14.2% and 13.3%, the investment cost (C_0) was in a range of \$1623–\$2641 per square meter PV area.

B. Tariff saving (s) and nominal increase rate (E)

Figure 5 plots the 2009–2015 tariffs and the yearly increasing rates of China Light and Power Company (CLP, 2015a) that supplied electricity to the project. A significant tariff increase from \$0.942 to \$1.110/kW was identified from 2011 to 2014. Given that the overall efficiency (η) of PV in operation ranged from 8.6% to 10.1%, the annual tariff saving (s) ranged from \$139 to \$163 per square meter PV panel area based on the latest tariff of \$1.141/kWh. Referring to tariff variations from 2009 to 2015, the nominal tariff increasing rate (E) with variations from 2.5% to 6% was considered in the subsequent analysis.

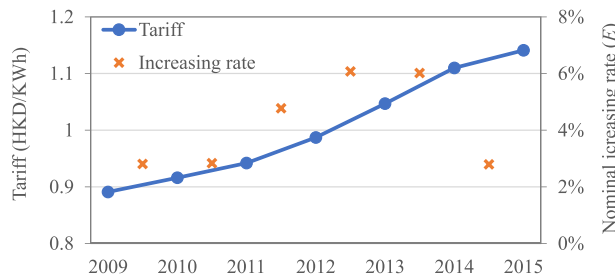


FIG. 5. The tariff and annual increasing rate of CLP from 2009 to 2015.

C. Carbon trading benefit (t)

The CO₂ emissions are the main source of greenhouse gas (GHG), and the reduction of these emissions produces additional revenues from the carbon trading. To estimate the CO₂ emission decline by PV panels, the local electricity production and CO₂ emissions from 2009 to 2015 of CLP were determined, which are given in Table II (2015a; 2015b). Since the electricity generations and CO₂ emissions varied moderately, the average carbon emission intensity (0.80 kg/kWh) in the 7 years from 2009 to 2015 was employed to estimate the annual decline of CO₂ emissions.

The price of carbon emission allowance, however, varied significantly in the past decade. The price of EU allowance fell from \$260/ton in 2008 to only \$43/ton in mid-2013 (Koch *et al.*, 2014) and ultimately \$26/ton in 2016 (Deeney *et al.*, 2016) because of policies, economic conditions, and the carbon emission certificates issued. The price in major cities of the United States and Mainland China of 2014 ranged from \$41/ton to \$86/ton (Tang *et al.*, 2015). In subsequent analysis, we evaluate the effect of the carbon trading price variations on the monetary payback period.

D. The maintenance cost (m), inflation rate (r_{inf}), and nominal interest rate (r)

The annual operation and maintenance cost (m) varied from 0.5% to 1.0% of the initial investment (Poullikkas, 2009 and Ramos and Ramos, 2009). The annual inflation rate (r_{inf}) was determined by the local consumer price index, which varied from 2% to 4.4% from 2007 to 2015 excluding the maximum and minimum values (Cen.Stat.Dep.HKSAR., 2014). The nominal interest rate (r) was found to vary from 0.5% to 0.75% according to the local base rate from 2009 to 2015 (HKMA, 2016). The ranges of different variables indicate different economic conditions, which in turn will result in different payback periods.

E. Sensitivity analysis

The monetary payback periods in various conditions can be difficult to depict because various variables may influence them. Sensitivity analysis can help to identify the relative importance of different variables (in terms of their influence) on the payback period. A sensitivity analysis analyzes how the model output variations can be apportioned to different sources of input variations (Saltelli *et al.*, 2000 and Sobol, 2001). The total sensitivity index of a variable is the percentage of output variations resulted from the variable itself and its combination with the other inputs. We estimated the sensitivity indexes of the uncertain variables, namely, C_0 , E , t , r_{inf} , r , and m , by the Extended Fourier Amplitude Sensitivity Test (E-FAST) (Saltelli *et al.*, 1999). E-FAST oscillates the input variables periodically at different frequencies, and the output variation is decomposed into a number of Fourier series that oscillate at positive integral frequencies. If an input variable has a strong effect on the output, the output oscillation at the corresponding frequency and its harmonics shall be of high amplitude (Cukier *et al.*, 1973 and Cukier *et al.*, 1978). By oscillating the variable of interest at a frequency significantly greater than the others, its effect on the model can be scaled by the output oscillation amplitudes at the correspondingly high frequencies. The approach accounts for the interactions between different variables and performances well for non-linear and non-monotonic problems. For our problem, the E-FAST process was implemented by the MATLAB code of Ekström (2005). Table III summarizes the ranges of tested variables according to Secs. IV A–IV D.

TABLE II. Electricity generation and CO₂ emissions of the local power station from 2009 to 2015.

Month	2009	2010	2011	2012	2013	2014	2015
Power generated (GWh)	24 920	24 552	24 955	24 102	25 084	25 597	24 075
CO ₂ (kton)	19 209	18 111	20 134	19 623	21 063	21 857	18 479

TABLE III. The variation ranges of variables being tested.

Parameter	C_0	E	η	m	r_{inf}	r
Minimum	\$1623/m ²	2.5%	8.6%	0.5% of C_0	2%	0.5%
Maximum	\$2641/m ²	6%	10.1%	1.0% of C_0	4.4%	0.75%

Figure 6 shows the total sensitivity index of the variables. It is not surprising that the payback period was most sensitive to the variation of C_0 and E with sensitivity indices over 0.7 and 0.1, respectively. The effect of t based on the carbon trading price of 2008 was slightly greater than the PV efficiency uncertainty. However, its impact varied by different assumptions and would reduce significantly based on the updated price after 2014. The reduction indicates that the PV installation incentive from carbon allowance trading was reducing steadily from 2008 to 2014. The sensitivity indices of C_0 , E , and t (after 2008) were greater than the PV panel efficiency (η). In subsequent studies, the payback periods at different C_0 , E , and t were analyzed when the other variables were kept as constant based on their sensitivity to the payback period.

F. Monetary payback periods

To get a better idea about the financial viability of the PV system, payback periods were determined based on the different values of the three most sensitive parameters (i.e., C_0 , E , and t). The year-round PV panel efficiency was assumed to be 9.35%, which corresponded to an energy production of 132 kWh/m² and \$151/m² savings based on the electricity tariff of 2015. The annual operation and maintenance cost (m) was 0.75% of C_0 . The inflation rate (r_{inf}) of 3.31% was the average consumer price index from 2006 to 2015. The nominal interest rate (r) of 0.75% was the latest base rate. Two carbon trading revenues (t) were considered: \$56/ton as the average of the maximum and minimum carbon trading price after 2014 and \$260/ton according to the price at 2008. Figure 7 shows the payback periods for these two different carbon trading revenues.

As shown in Fig. 7(a), the monetary payback period of PV in Hong Kong varied from 9 to 16.8 years based on different C_0 and E values and the updated carbon emission price. Greater E and lower C_0 would lead to shorter investment payback periods. The influence of E on the payback period was significant at high C_0 . The period varied from 13.4 to 16.8 years for different E values when C_0 per Watt was kept constant at \$19. For C_0 per Watt as low as \$12, the effect of E on the period was less significant, which ranged from about 9 to 10.5 years. The results indicate a significant effect of C_0 and a moderate effect of E on the PV monetary payback periods. Since C_0 would reduce while E may increase in the future in Hong Kong, the payback period of the monetary investment would be shorter and the monetary benefits would be

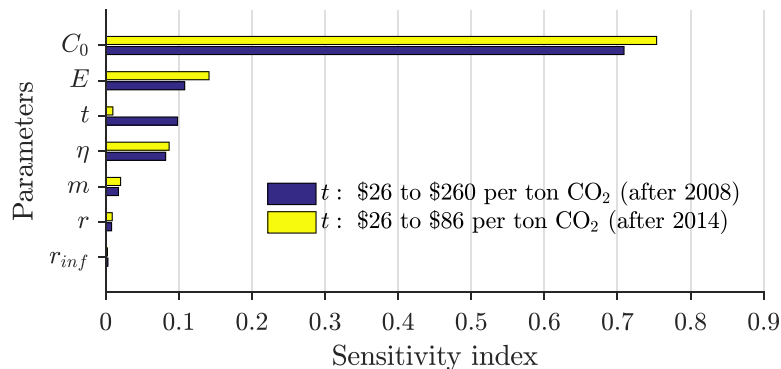


FIG. 6. The sensitivity of the payback period to variable variations.

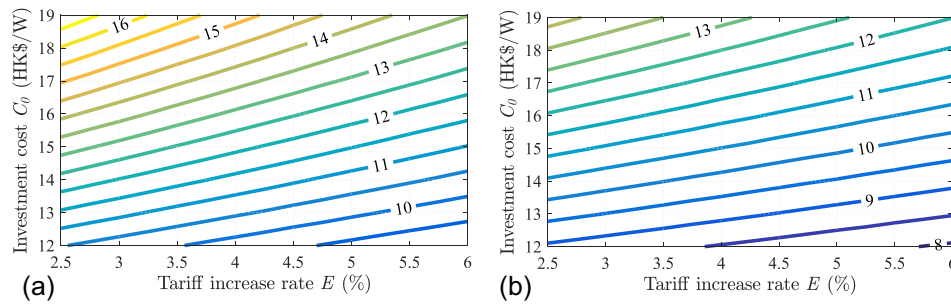


FIG. 7. (a) The investment payback periods (years) at different tariff increase rates and initial cost when the price of carbon emission allowance was \$56/ton. (b) The investment payback periods (years) at different tariff increase rates and initial cost when the price of carbon emission allowance was \$260/ton.

greater. The differences between the monetary payback periods in Figs. 7(a) and 7(b) show the impact of carbon emission allowance trading on the monetary payback period of PV. The payback period in Fig. 7(b) under a more favorable price of carbon emission trade was 1.2–2.9 years less (13%–17% less) compared with Fig. 7(a). The decline was moderate and close to the variation due to E variations, which was consistent with the sensitivity analysis shown in Fig. 6. With carbon trading benefit reduced from \$260/ton to about \$56/ton, the carbon trading would no longer be an effective tool to encourage the PV system installation.

G. Energy and greenhouse gas payback periods

The embodied energy payback period is the time the PV system will take to generate energy equivalent to the embodied energy of PV manufacturing (E_{em}). The payback period of embodied energy is necessary to judge whether the PV system is energy positive. E_{em} includes the energy demands for metallurgical and electronic grade silicon production, Czochralski process, slicing, cell and module production, transportation, array supporting, cabling, and inverter. Recent studies (Alsema and de Wild-Scholten, 2006; Laleman *et al.*, 2011; and Nawaz and Tiwari, 2006) showed that the average embodied energies of monocrystalline PV cells and balance of system (BOS) items were 1137 kWh/m² and 358 kWh/m², respectively. The BOS includes the inverter, controller, and array support. The modules of sites A and B were manufactured in Shanghai and Singapore, which are 1930 km and 2610 km away from the site in Hong Kong, respectively. So, the transportation energy was 1.52 kWh/m² and 2 kWh/m² according to 0.0002 MJ/(km kg) of deep sea transport (EMSD, 2006). The total embodied energy of PV panels in sites A and B was approximately 1497 kWh/m². Considering the annual degradation rate of power generation as 0.5%, the payback period of embodied energy was 10.8 and 12.7 years for PV in sites A and B, respectively. This was less than the monetary payback periods of under most conditions based on the current carbon trading benefit, as shown in Fig. 7(a). The net energy ratio (Akinyele and Rayudu, 2016c), defined as the times of PV energy output for PV cell manufacture during the 20–30-year PV cell lifespan, was 1.81–2.65 for site A and 1.55–2.26 for site B.

Similarly, the environmental benefit of PV is the period of restoring the embodied GHG of the PV system by the annual GHG reduction due to less fossil fuel consumption. The embodied GHG of the PV system includes 463 kg CO₂eq/m² for PV cell fabrication (Battisti and Corrado, 2005), 125 kg CO₂eq/m² for inverters, and 6.1 kg CO₂eq/m² for array supporting and cabling (Alsema and de Wild-Scholten, 2006). The total embodied GHG was found to be 594.1 kg CO₂eq/m², indicating that the GHG per lifecycle energy outputs were 149.5–218.9 gCO₂eq/kWh for site A and 175.2–256.6 gCO₂eq/kWh for site B for the 20–30-year lifespan. Given that the annual CO₂ emission decrease was 98 kg/m²–114 kg/m² and a degradation rate of 0.5% per year, the GHG payback period was 5.3–6.2 years for the two sites. This was far shorter than the embodied energy and monetary investment payback periods.

The payback periods of both greenhouse gas and embodied energy were found to be lower than the life span of PV panels, which is usually assumed to be 20–30 years (Geem, 2012 and Sharma and Tiwari, 2013). Thus, the PV system can be effective to produce energy and reduce carbon emission. Although the momentary payback period was much longer compared with embodied energy and greenhouse gas, the difference can be narrowed down by greater carbon trading benefits (t) and electricity tariff increase rates (E). The much longer monetary payback period is because of the cost of the labor force in PV manufacturing and retailing and the low benefit of carbon trading. The cost of carbon emission (i.e., carbon footprint) has not been fully included in the current electricity tariff nor the carbon trading benefits. Considering the growing awareness of global warming and climate change among the public, the carbon footprint is likely to be a major factor considered by policy makers in the energy sector and a further increase in the cost of electricity would be expected. It is envisaged that the monetary payback period of PV would reduce accordingly and be comparable to the embodied energy and carbon emission payback periods.

V. CONCLUSIONS

The operating performance of two rooftop photovoltaic systems in Hong Kong was studied by the on-site measurements from 2011 to 2015. The monthly average daily solar irradiance peaked at 5366 Wh/m² in August. The corresponding electricity production peaked at 429 Wh/m² and 485 Wh/m² for different installations. Regarding energy conversion, the overall efficiencies of PV panels in various sites ranged from 8.6% to 10.1%, which were less than the standard test conditions. The annual electricity generation of the two sites ranged from 122 kWh/m² to 143 kWh/m². The sensitivity analysis showed that the monetary payback period of PV was most sensitive to the initial investment cost and electricity tariff increase rate. Based on the current trading benefit of carbon emission set in 2014, it would take 9–16.8 years to recover the initial investments by the benefits. The payback period would be 1.2–2.9 years less under the more favorable carbon emission trade price of 2008. PV installations could be encouraged by shorter monetary payback periods at lower investment cost, a greater increase rate of electricity tariff, and more considerable carbon trading benefits. The estimated embodied energy and greenhouse gas payback periods were 10.8–12.7 and 5.3–6.2 years, respectively. These payback periods are well below the life span of PV systems. The monetary payback period would be comparable to the embodied energy and carbon emission payback periods if the carbon footprint is considered in the electricity tariff or the carbon trading benefits. With the likely increase in the electricity tariff and the gradual reduction in the PV installation cost, we believe that PV systems would become more attractive both financially and environmentally. Future work will analyse the PV cell efficiency variations in the actual outdoor environment and correlate the efficiency with accessible indices such as cell temperature.

ACKNOWLEDGMENTS

The work described in this paper was fully supported by a General Research Fund from the Research Grant Council of the Hong Kong Special Administrative Region, China [Project No. 9041470 (CityU 117209)]. The part of the PV power production data was provided by Ho Koon Nature Education cum Astronomical Center (HKNEAC). Siwei Lou was supported by a City University of Hong Kong studentship.

- Akinyele, D. O., "Environmental performance evaluation of a grid-independent solar photovoltaic power generation (SPPG) plant," *Energy* **130**, 515–529 (2017).
- Akinyele, D. O. and Rayudu, R. K., "Community-based hybrid electricity supply system: A practical and comparative approach," *Appl. Energy* **171**, 608–628 (2016a).
- Akinyele, D. O. and Rayudu, R. K., "Strategy for developing energy systems for remote communities: Insights to best practices and sustainability," *Sustainable Energy Technol. Assess.* **16**, 106–127 (2016b).
- Akinyele, D. O. and Rayudu, R. K., "Techno-economic and life cycle environmental performance analyses of a solar photovoltaic microgrid system for developing countries," *Energy* **109**, 160–179 (2016c).
- Alsema, E. A. and de Wild-Scholten, M. J. "Environmental impacts of crystalline silicon photovoltaic module production," in *The 13th CIRP International Conference on Life Cycle Engineering*, Leuven (2006).

- Barbose, G., Darghouth, N., Millstein, D., Spears, M., and Wiser, R., *Tracking the Sun VIII: The Installed Price of Residential and Non-Residential Photovoltaic Systems in the United States* (Lawrence Berkeley National Laboratory, 2015).
- Battisti, R. and Corrado, A., "Evaluation of technical improvements of photovoltaic systems through life cycle assessment methodology," *Energy* **30**, 952–967 (2005).
- Bhakta, S., Mukherjee, V., and Shaw, B., "Techno-economic analysis of standalone photovoltaic/wind hybrid system for application in isolated hamlets of North-East India," *J. Renewable Sustainable Energy* **7**, 023126 (2015).
- Cen.Stat.Dep.HKSAR., *Annual Report on the Consumer Price Index 2013* (Census and Statistics Department HKSAR, Hong Kong, 2014).
- CLP, *Annual Report* (CLP, Hong Kong, 2015a).
- CLP, *Sustainability Report* (CLP, Hong Kong, 2015b).
- Cukier, R. I., Fortuin, C. M., Shuler, K. E., Petschek, A. G., and Schaibly, J. H., "Study of the sensitivity of coupled reaction systems to uncertainties in rate coefficients. I. Theory," *J. Chem. Phys.* **59**, 3873–3878 (1973).
- Cukier, R. I., Levine, H. B., and Shuler, K. E., "Nonlinear sensitivity analysis of multiparameter model systems," *J. Comput. Phys.* **26**, 1–42 (1978).
- Deeney, P., Cummins, M., Dowling, M., and Smeaton, A. F., "Influences from the European Parliament on EU emissions prices," *Energy Policy* **88**, 561–572 (2016).
- Ekström, P. A., *Ekios: A Simulation Toolbox for Sensitivity Analysis* (Uppsala University, Sweden, 2005).
- EMSD, *Consultancy Study on Life Cycle Energy Analysis of Building Construction - Final Report* (EMSD, Hong Kong, 2006).
- EMSD, *An Introduction to Life Cycle Energy Assessment (LCEA) of Building Developments* (EMSD, Hong Kong, 2007).
- EMSD, *Energy Utilization Indexes and Benchmarks for Residential, Commercial and Transport Sectors* (Electrical and Mechanical Services Department, 2016).
- Environment Bureau, *Energy Saving Plan for Hong Kong's Built Environment 2015-2025+* (Environment Bureau, Hong Kong, 2015).
- Geem, Z. W., "Size optimization for a hybrid photovoltaic–wind energy system," *Int. J. Electr. Power Energy Syst.* **42**, 448–451 (2012).
- Hasanuzzaman, M., Al-Amin, A. Q., Khanam, S., and Hosenuzzaman, M., "Photovoltaic power generation and its economic and environmental future in Bangladesh," *J. Renewable Sustainable Energy* **7**, 013108 (2015).
- Hennecke, A. M., Faist, M., Reinhardt, J., Junquera, V., Neeft, J., and Fehrenbach, H., "Biofuel greenhouse gas calculations under the European renewable energy directive—A comparison of the BioGrace tool vs. the tool of the roundtable on sustainable biofuels," *Appl. Energy* **102**, 55–62 (2013).
- HKMA, *Annual Report* (Hong Kong Monetary Authority, Hong Kong, 2016).
- Islam, M. R., Mekhilef, S., and Saidur, R., "Progress and recent trends of wind energy technology," *Renewable Sustainable Energy Rev.* **21**, 456–468 (2013).
- Jordan, D. C. and Kurtz, S. R., "Photovoltaic degradation rates—an analytical review," *Prog. Photovoltaics Res. Appl.* **21**, 12–29 (2013).
- Koch, N., Fuss, S., Godefroy, G., and Edenhofer, O., "Causes of the EU ETS price drop: Recession, CDM, renewable policies or a bit of everything?—New evidence," *Energy Policy* **73**, 676–685 (2014).
- Kolokotsa Kolhe, M., Kolhe, S., and Joshi, J. C., "Economic viability of stand-alone solar photovoltaic system in comparison with diesel-powered system for India," *Energy Econ.* **24**, 155–165 (2002).
- Laleman, R., Albrecht, J., and Dewulf, J., "Life cycle analysis to estimate the environmental impact of residential photovoltaic systems in regions with a low solar irradiation," *Renewable Sustainable Energy Rev.* **15**, 267–281 (2011).
- Lam, J. C. and Li, D. H. W., "Correlation between global solar radiation and its direct and diffuse components," *Build. Environ.* **31**, 527–535 (1996).
- Li, D. H. W., Cheung, K. L., Lam, T. N. T., and Chan, W., "A study of grid-connected photovoltaic (PV) system in Hong Kong," *Appl. Energy* **90**, 122–127 (2012).
- Li, D. H. W., Chow, S. K. H., and Lee, E. W. M., "An analysis of a medium size grid-connected building integrated photovoltaic (BIPV) system using measured data," *Energy Build.* **60**, 383–387 (2013a).
- Li, D. H. W. and Lam, T. N. T., "Determining the optimum tilt angle and orientation for solar energy collection based on measured solar radiance data," *Int. J. Photoenergy* **2007**, 85402.
- Li, D. H. W., Lou, S. W., and Lam, J. C., "An analysis of global, direct and diffuse solar radiation," *Energy Procedia* **75**, 388–393 (2015).
- Li, D. H. W., Yang, L., and Lam, J. C., "Zero energy buildings and sustainable development implications—A review," *Energy* **54**, 1–10 (2013b).
- Nawaz, I. and Tiwari, G. N., "Embodied energy analysis of photovoltaic (PV) system based on macro- and micro-level," *Energy Policy* **34**, 3144–3152 (2006).
- Oliver, J. G. J., Janssens-Maenhout, G., Muntean, M., and Peters, J. A. H. W., *Trends in Global CO2 Emissions 2015* (PBL Netherlands Environmental Assessment Agency, The Hague, Netherlands, 2015).
- Poullikkas, A., "Parametric cost-benefit analysis for the installation of photovoltaic parts in the island of Cyprus," *Energy Policy* **37**, 3673–3680 (2009).
- Ramos, J. S. and Ramos, H. M., "Sustainable application of renewable sources in water pumping systems: Optimized energy system configuration," *Energy Policy* **37**, 633–643 (2009).
- Saltelli, A., Chan, K., and Scott, E. M., *Sensitivity Analysis: Gauging the Worth of Scientific Models* (Wiley, Chichester, 2000).
- Saltelli, A., Tarantola, S., and Chan, K. P. S., "A quantitative model-independent method for global sensitivity analysis of model output," *Technometrics* **41**, 39–56 (1999).
- Sharma, R. and Tiwari, G. N., "Life cycle assessment of stand-alone photovoltaic (SAPV) system under on-field conditions of New Delhi, India," *Energy Policy* **63**, 272–282 (2013).
- Shukla, P. R. and Chaturvedi, V., "Low carbon and clean energy scenarios for India: Analysis of targets approach," *Energy Econ.* **34**(Suppl 3), S487–S495 (2012).

- Skoplaki, E. and Palyvos, J. A., "On the temperature dependence of photovoltaic module electrical performance: A review of efficiency/power correlations," [Sol. Energy](#) **83**, 614–624 (2009).
- Sobol, I. M., "Global sensitivity indices for nonlinear mathematical models and their Monte Carlo estimates," [Math. Comput. Simul.](#) **55**, 271–280 (2001).
- Sweeney, J. F., Pate, M. B., and Choi, W., "Life cycle production and costs of a residential solar hot water and grid-connected photovoltaic system in humid subtropical Texas," [J. Renewable Sustainable Energy](#) **8**, 053702 (2016).
- Tang, L., Wu, J., Yu, L., and Bao, Q., "Carbon emissions trading scheme exploration in China: A multi-agent-based model," [Energy Policy](#) **81**, 152–169 (2015).
- To, W. M., Lai, T. M., Lo, W. C., Lam, K. H., and Chung, W. L., "The growth pattern and fuel life cycle analysis of the electricity consumption of Hong Kong," [Environ. Pollut.](#) **165**, 1–10 (2012).
- Wong, M. S., Zhu, R., Liu, Z., Lu, L., Peng, J., Tang, Z., Lo, C. H., and Chan, W. K., "Estimation of Hong Kong's solar energy potential using GIS and remote sensing technologies," [Renewable Energy](#) **99**, 325–335 (2016).